Chemical Science

RSC Publishing

EDGE ARTICLE

View Article Online
View Journal | View Issue

Published on 18 December 2012. Downloaded by Michigan State University on 19/01/2016 01:38:51.

Cite this: *Chem. Sci.*, 2013, **4**, 1028

# Switching with orthogonal stimuli: electrochemical ring-closure and photochemical ring-opening of bis(thiazolyl)maleimides†

Martin Herder,[a] Manuel Utecht,[b] Nicole Manicke,[a] Lutz Grubert,[a] Michael Pätzel,[a] Peter Saalfrank*[b] and Stefan Hecht*[a]

Received 5th October 2012
Accepted 24th November 2012

DOI: 10.1039/c2sc21681g

**www.rsc.org/chemicalscience**

The photochemistry as well as electrochemistry of novel donor–acceptor bis(morpholinothiazolyl)–maleimides has been investigated. Proper substitution of these diarylethene-type molecular switches leads to the unique situation in which their ring-closure can only be accomplished electrochemically, while ring-opening can only be achieved photochemically. Hence, these switches operate with orthogonal stimuli, *i.e.* redox potential and light, respectively. The switch system could be optimized by introducing trifluoromethyl groups at the reactive carbon atoms in order to avoid by-product formation during oxidative ring closure. Both photochemical and electrochemical pathways were investigated for methylated, trifluoromethylated, and nonsymmetrical bis(morpholinothiazolyl)maleimides as well as the bis(morpholinothiazolyl)cyclopentene reference compound. With the aid of the nonsymmetrical "mixed" derivative, the mechanism of electrochemically driven ring closure could be elucidated and seems to proceed *via* a dicationic intermediate generated by two-fold oxidation. All experimental work has been complemented by density functional theory that provides detailed insights into the thermodynamics of the ring-open and closed forms, the nature of their excited states, and the reactivity of their neutral as well as ionized species in different electronic configurations. The particular diarylethene systems described herein could serve in multifunctional (logic) devices operated by different stimuli (inputs) and may pave the way to converting light into electrical energy *via* photoinduced "pumping" of redox-active meta-stable states.

## Introduction

Chemists are continuously challenged to construct and to manipulate increasingly complex functional systems and materials. For this purpose one central prerequisite is the ability to influence the properties of the whole molecular ensemble by gaining precise control over the behaviour of its single building blocks. One attractive way to accomplish this is the use of molecular units that can be "switched" between two forms associated with different physicochemical properties by an external stimulus. Particularly, the incorporation of photochromic molecules into complex functional systems, in combination with the use of light as a noninvasive stimulus with high spatial and temporal resolution, has recently gained much attention.[1]

Among these photochromic compounds diarylethenes belong to the most promising candidates as they typically offer an efficient isomerization behaviour and a high fatigue resistance.[2] Besides the modulation of optical properties useful for information storage and processing,[3] they are exploited as functional units for remote-controlling electronic devices,[4] chemical reactivity,[5] and supramolecular binding and aggregation.[6]

Another interesting feature of diarylethenes is the possibility of triggering their isomerization reaction not only by light but also by electrochemical oxidation or reduction (Scheme 1). Thus, it was reported that diarylethenes bearing thiophenes as aryl moieties (dithienylethenes, DTEs) can undergo oxidative cyclization or cycloreversion depending on the substitution pattern.[7] A similar behaviour was also reported for DTEs substituted with redox-active metal centres.[8] An isomerization

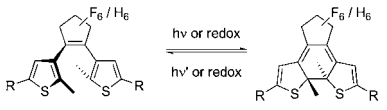


**Scheme 1** Isomerization of dithienylethenes.

[a]*Department of Chemistry, Humboldt-Universität zu Berlin, Brook-Taylor-Str. 2, 12489 Berlin, Germany. E-mail: sh@chemie.hu-berlin.de*

[b]*Institut für Chemie, Universität Potsdam, Karl-Liebknecht-Str. 24-25, 14476 Potsdam-Golm, Germany. E-mail: peter.saalfrank@uni-potsdam.de*

† Electronic supplementary information (ESI) available: Experimental details including synthesis, photochemistry, electrochemistry, and computational methods and data. See DOI: 10.1039/c2sc21681g



This journal is © The Royal Society of Chemistry 2013

Published on 18 December 2012. Downloaded by Michigan State University on 19/01/2016 01:38:51.

from the ring-open to the ring-closed isomer upon electrochemical reduction was observed for diarylethenes substituted with two cationic *N*-methylpyridinium units in the periphery.[9] The combination of the different strategies in one molecular scaffold afforded a fully bidirectional switchable compound that undergoes isomerization in both directions either by excitation with light or by the electrochemical pathway.[10] Nevertheless, to the best of our knowledge, *separation* of the electrochemical and the photochemical pathways for the isomerization of diarylethenes in order to precisely control the state of the switching molecule using either one of the two stimuli has never been achieved.

While the photochemistry of diarylethenes has been exploited extensively in terms of understanding their general mechanism of operation and tuning the system in order to gain maximum isomerization efficiencies[11] and fatigue resistance,[12] there have been few systematic studies concerning the isomerization reaction *via* the electrochemical pathway.[13] Thus, it is still necessary to gain deeper experimental and theoretical insight into the fundamental principles of the electrochemical isomerization of diarylethenes as well as to optimize it in terms of efficiency and fatigue resistance in order to combine the photochemical and the electrochemical switching processes in sophisticated functional systems.

Here we report the oxidative isomerization of diarylethenes that bear thiazole moieties instead of the commonly utilized thiophenes. Thiazoles as aromatic moieties for the construction of diarylethenes offer, besides their good synthetical availability, advantages in terms of thermal and photochemical stability.[14] Specifically, species **1–4**, as shown in Scheme 2, were studied, with **a** referring to open and **b** to closed forms, respectively. While until now no oxidative isomerization of such dithiazolylethenes has been reported in the literature, our system possesses an orthogonal behaviour towards both switching stimuli, *i.e.* the electrochemical switching only operates for the ring-closure and the photochemical pathway is only possible for the ring-opening reaction. A central prerequesite for achieving the orthogonality is the utilization of highly electron donating morpholino substituents on the thiazole rings in combination with a highly electron deficient maleimide as the bridging unit. It is shown that the stability of **1a** during the switching process can be enhanced significantly by the introduction of trifluoromethyl groups in the 5- and 5′-position of the thiazole rings leading to structure **2a**. The nonsymmetrically substituted derivative **3a** provides distinct experimental evidence for the mechanism of the oxidative ring-closing process. As a reference compound **4a**, possessing an electron-neutral cyclopentene bridge, was synthesized, which shows both electrochemical and photochemical cyclization. In addition to experimental results, theoretical calculations based on density functional theory (DFT) were performed in order to gain further insight into the absorption behaviour, ground and excited state structures, reaction pathways, as well as transition states for neutral and ionic species.

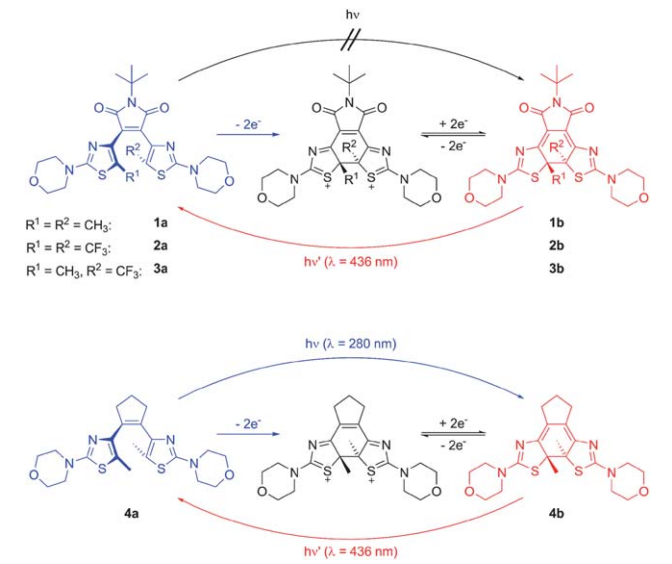


**Scheme 2** Isomerization behaviour of morpholino-substituted dithiazolylethenes.

## Results and discussion

### Synthesis

Synthesis of compounds **1a–4a** relied on the established strategy of connecting the aryl moieties to the bridge moiety by cross-coupling (Scheme 3). 5-Methyl-2-morpholinothiazole **6** was easily accessed *via* Hantzsch's thiazole synthesis. The trifluoromethylated analogue **10** was accessed by iodination of the 5-unsubstituted thiazole precursor and subsequent copper-catalysed trifluoromethylation using $TMSCF_3$[15] in moderate yields. Both compounds could be converted into the corresponding organostannanes **7** and **11** by direct metalation using *tert*-BuLi und subsequent quenching with $Bu_3SnCl$. Finally, Stille cross-coupling of **7** or **11** either with 3,4-dibromo-1-*tert*-butylmaleimide **8** or with 1,2-dibromocyclopentene **12** yielded the symmetrically substituted dithiazolylethenes **1a**, **2a**, and **4a**, respectively. The nonsymmetrically substituted derivative **3a** was accessed *via* a statistical reaction of both organostannanes with maleimide **8** under the same conditions.

The ring-closed isomer **1b** was obtained by oxidation of an acetonitrile solution of **1a** using two equivalents of ceric ammonium nitrate and subsequent reduction with sodium ascorbate, followed by purification using preparative HPLC. Compounds **2b** and **4b** were isolated by controlled potential electrolysis of acetonitrile solutions of the respective ring-open isomers and subsequent purification of the crude mixtures by precipitation or by chromatography.

### Photochemical behaviour

UV/vis-spectra of ring-open compounds **1a**, **2a**, **3a**, and **4a** were recorded in acetonitrile (Fig. 1). Besides an intense absorption in the UV originating from the aromatic thiazole moieties, the structurally related compounds **1a**, **2a**, and **3a** show a broad absorption band in the visible range between 350–500 nm. This band can be attributed to the charge-transfer from the electron-rich morpholinothiazoles to the strongly electron-deficient

Published on 18 December 2012. Downloaded by Michigan State University on 19/01/2016 01:38:51.

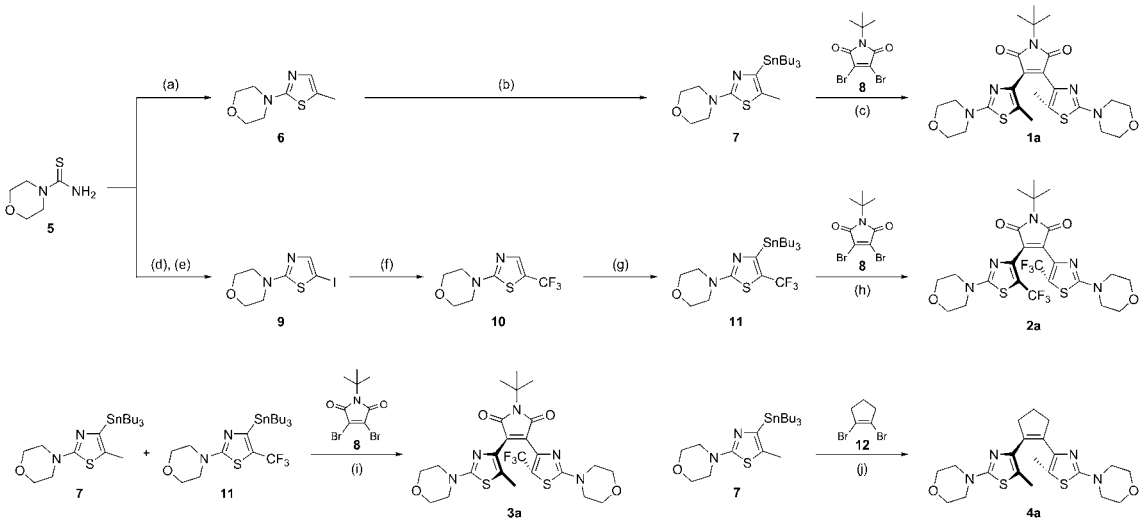

**Scheme 3** Synthesis of target photochromes **1a**, **2a**, **3a**, and **4a**: (a) 2-bromo-1,1-diethoxypropane, TsOH, (EtOH/$H_2O$), 90 °C, 24 h, 55%; (b)(i) *tert*-BuLi, (THF), −78 °C, 35 min, (ii) $Bu_3SnCl$, (THF), −78 °C to rt, 1 h, quant.; (c) **8**, $Pd_2(dba)_3$, $AsPh_3$, CuI, (DMF), rt, 6 h, 33%; (d) 2-bromo-1,1-diethoxyethane, TsOH, (EtOH/$H_2O$), 90 °C, 24 h, 97%; (e)(i) *n*-BuLi, (THF), −78 °C to −10 °C, 30 min, (ii) $I_2$, (THF), −10 °C, 30 min, 84%; (f) $TMSCF_3$, CuI, KF, (DMF/NMP), 50 °C, 4.5 h, 36%; (g)(i) *tert*-BuLi, (THF), −78 °C, 25 min, (ii) $Bu_3SnCl$, (THF), −78 °C to rt, 1 h, quant.; (h) **8**, $Pd(PPh_3)_4$, (toluene), 110 °C, 24 h, 29%; (i) **8**, $Pd(PPh_3)_4$, (toluene), 100 °C, 48 h, 3%; (j) **12**, $PdCl_2(PPh_3)_2$, (DMF), 100 °C, 20 h, 6%.

*tert*-butylmaleimide bridge. Compared to the parent structure **1a**, for compounds **2a** and **3a** the intensity of this CT-band is significantly lower and its position is shifted hypsochromically by 40 nm and 10 nm, respectively, reflecting the reduced electron-density of the $CF_3$-substituted morpholinothiazole cores.

As proposed in the literature for analogous dithienylmaleimides,[16] such a pronounced CT-behaviour between the aryl moieties and the bridge moiety of diarylethenes can lead to a diminished cyclization efficiency due to the formation of a Twisted Intramolecular Charge Transfer (TICT) excited state, which is characterized by a pronounced twisting of the single bond between the electron donating and the electron accepting parts of the molecule.[17] In fact, during irradiation of a yellow solution of **1a** in acetonitrile with UV-light ($\lambda_{irr}$ = 280 nm) or with visible light ($\lambda_{irr}$ = 436 nm) no changes in the UV/vis-spectrum could be observed (Fig. 1a). Furthermore, analysis of the reaction mixture by ultra-performance liquid chromatography (UPLC) did not show any new photoproduct. Only when exposed to UV-irradiation over an extended time period using a high intensity lamp some unspecific degradation (bleaching) took place. According to the TICT-model, the usage of cyclohexane as a non-polar solvent allowed for the photochemical cyclization reaction to take place to some extent. Nevertheless, its efficiency was extremely low with a quantum yield of 0.05 for the ring-closure of **1a** and a conversion of only 16% in the photostationary state (see Section 2 in the ESI†). A similar lack of photochemical reactivity for the ring-open isomers was also observed for the $CF_3$-substituted derivatives **2a** and **3a**.

Nevertheless, the ring-closed isomers **1b** and **2b** could be obtained *via* oxidation of the respective ring-open isomers (*vide infra*). They show an intense absorption in the visible region split into two bands (Fig. 1a and b insets). Upon illumination of acetonitrile solutions of **1b** and **2b** with visible light ($\lambda_{irr}$ = 436 nm) both bands diminish rapidly and the spectra of the respective ring-open compounds are obtained. Although the spectra of the ring-closed and the ring-open isomers overlap significantly at the irradiation wavelength, complete conversion to the ring-open isomers is achieved, as these are photochemically inactive. The quantum yields for the ring-opening of **1b** and **2b** with 436 nm light were determined to be relatively high with values of 0.13 and 0.37, respectively. Noticably, the ring-opening process is significantly enhanced for compound **2b**, which may be attributed to the strong electron-withdrawing character of the $CF_3$-groups attached to the reactive carbon atoms.[18]

Contrasting this unidirectional photochemical switching behaviour of diarylethenes **1a/b**, **2a/b**, and **3a/b**, bearing a maleimide bridge, compound **4a/b**, possessing a cyclopentene as bridging unit, shows photochemical bidirectionality to some extent (Fig. 1d). UV/vis spectra as well as UPLC-traces recorded during irradiation of a colorless solution of **4a** in acetonitrile with UV-light ($\lambda_{irr}$ = 280 nm) indicate the formation of the ring-closed isomer **4b**. However, only 36% of **4b** is formed in the photostationary state due to a high ring-opening quantum yield of 0.26 while the ring-closing quantum yield was determined to be 0.13. Obviously the lack of a charge transfer between the thiazole moieties and the cyclopentene bridge, indicated by the absence of a visible absorption in the case of the ring-open isomer, restores the reversibility of the photochemical reaction typical for diarylethenes. Taking all of these data summarized in Table 1 into consideration, an intramolecular charge transfer interaction is clearly essential to install unidirectional photochemical behaviour.

To get further insight into the photochemical processes that lead to the observed lack of cyclization efficiency theoretical investigations were performed. We optimized the structures of compounds **1a–4b** on the B3LYP/6-31G*[19] and CAM-B3LYP/6-31G*[20] levels of theory. Solvent effects were modeled using the

 This journal is © The Royal Society of Chemistry 2013

Published on 18 December 2012. Downloaded by Michigan State University on 19/01/2016 01:38:51.

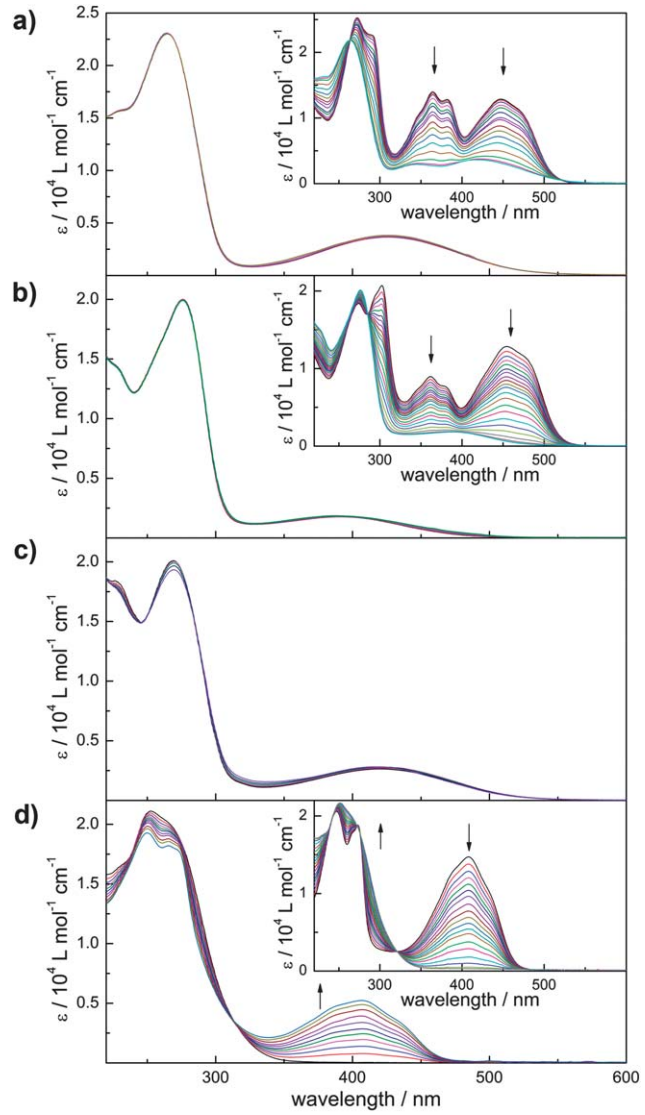


**Fig. 1** UV/vis-spectra during the course of irradiation of acetonitrile solutions of (a) **1a**, (b) **2a**, (c) **3a**, and (d) **4a** with UV-light ($\lambda_{irr}$ = 280 nm). Insets show UV/vis spectra during the irradiation with visible light ($\lambda_{irr}$ = 436 nm) of the respective isolated ring-closed isomers **1b**, **2b**, and **4b** (prepared separately *via* oxidation of the ring-open compounds) in acetonitrile. All concentrations 5 × $10^{-5}$ M.

*Polarizable Continuum Model* (PCM).[21] UV/vis absorption spectra were calculated using linear-response time-dependent DFT (TD-DFT)[22] on the TD-CAM-B3LYP level of theory, by broadening vertical stick spectra with Gaussians of width 1500 $cm^{-1}$. All results were obtained using the GAUSSIAN09 program package.[23] Further computational details can be found in the ESI.† In Fig. 2 the broadened spectra of **1a–4b** with acetonitrile as a solvent are shown, as obtained from TD-CAM-B3LYP/PCM/6-31G* calculations. Selected wavelengths, oscillator strengths, and characters of the most intense transitions at wavelengths above 240 nm are listed in Table S2 of the ESI.†

The calculated wavelengths of transitions are overall hypsochromically shifted compared to experimental values, but otherwise nicely confirm the experimentally observed trends. The overall shift is rather constant with values between about 10 and 35 nm for the ring-open isomers and between 40 and 60 nm for the ring-closed isomers. This blue-shift is due, in part, to a slight overestimation of excitation energies by TD-CAM-B3LYP, and due to the idealization of the solvent as a continuum in the PCM. By contrast, the TD-B3LYP method underestimates excitation energies considerably (see Section 9 in the ESI†), due to a wrong asymptotic one-electron potential, which is corrected for in the CAM-B3LYP functional.[20] As a consequence, the CAM-B3LYP functional is more reliable for charge transfer excitations, which are of importance here.

In particular, the TD-CAM-B3LYP spectra reproduce the weak, broad band for the ring-open forms **1a–3a** at around 400 nm (and slightly below), which is due to a charge transfer from the thiazole units to the central maleimide bridge. This assignment is supported by the fact that for **1a–3a** the lowest-energy transition is of the HOMO → LUMO type, where HOMO and LUMO are localized at the thiazole and maleimide units, respectively, as is exemplarily shown for compound **1a** (Fig. 3, left). The calculations also confirm the strong blue-shift of the CT band of compound **2a** relative to **1a**, and the much weaker blue-shift for species **3a**. These hypsochromically shifted transitions are due to two and one electron-withdrawing $CF_3$-groups, respectively, which lower the HOMO energy. The CT transition is suppressed both in theory and experiment for compound **4a**, since cyclopentene as a bridging unit is only a weak electron acceptor (Fig. 3, right). As a consequence, there is no absorption of **4a** at wavelengths above 300 nm, neither experimentally nor theoretically. In the UV regime (at around 260 nm according to experiment and 240 nm in theory), the morpholinothiazole groups of the ring-open compounds show strong absorption. In further agreement between theory and experiment, the ring-closed compounds **1b–4b** show considerable overlap with the spectra of open forms **1a–4a**. For **1b–3b**,

**Table 1** Photophysical properties for acetonitrile solutions of ring-open isomers **1a**, **2a**, **3a**, and **4a** as well as isolated ring-closed isomers **1b**, **2b**, and **4b**

| | $\lambda_{max}$ [nm] ($\varepsilon$ [$10^3$ L $mol^{-1}$ $cm^{-1}$]) | | | | |
|---|---|---|---|---|---|
| Comp. | Ring-open isomer | Ring-closed isomer | $\Phi_{o\rightarrow c}$ (280 nm) | $\Phi_{c\rightarrow o}$ (436 nm) | Conversion[a] (280 nm) |
| **1a/b** | 265 (23.1), 430 (3.9) | 364 (14.0), 447 (12.9) | <0.001 | 0.13 | <1% |
| **2a/b** | 276 (20.1), 390 (1.8) | 361 (8.9), 454 (12.9) | <0.001 | 0.37 | <1% |
| **3a/b** | 269 (18.9), 420 (2.5) | n.d.[b] | <0.001 | n.d.[b] | <1% |
| **4a/b** | 252 (21.1), 268 (shoulder) | 408 (14.7) | 0.13 | 0.26 | 36% |

[a] Amount of ring-closed isomer in the photostationary state upon irradiation with UV-light determined by UPLC. [b] Compound **3b** was not isolated.

Published on 18 December 2012. Downloaded by Michigan State University on 19/01/2016 01:38:51.

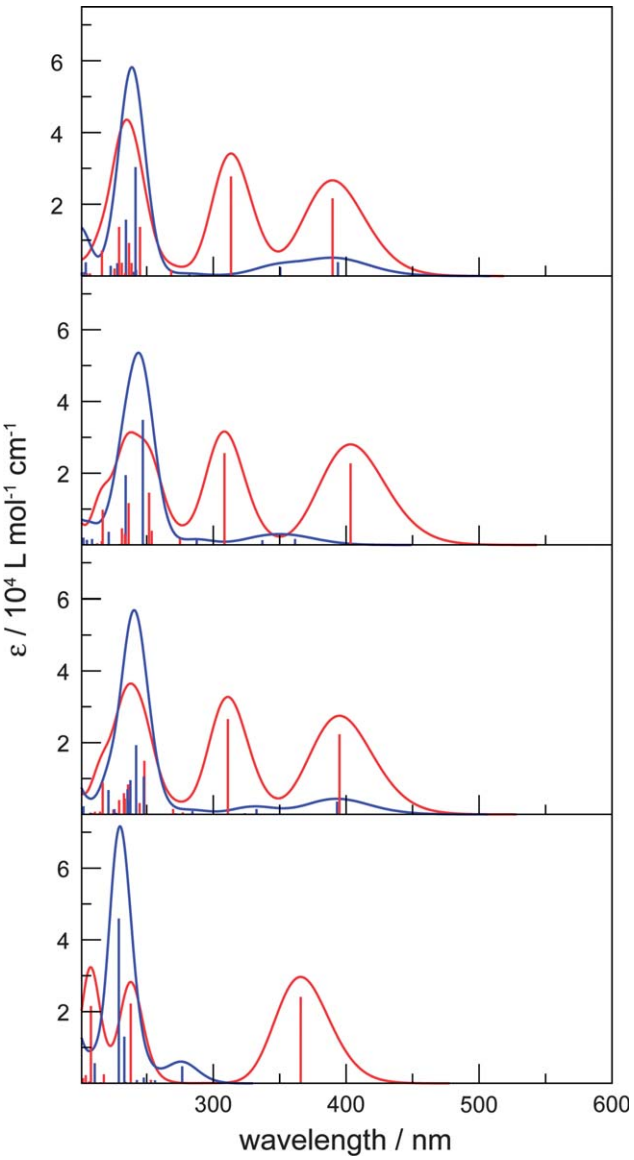


**Fig. 2** Calculated absorption spectra of **1–4** (**a** in blue and **b** in red) in acetonitrile on the TD-CAM-B3LYP/PCM/6-31G* level of theory. Line spectra (sticks) are broadened by Gaussians of 1500 $cm^{-1}$ width.

the spectra are dominated by three well-separated bands. The lowest-energy HOMO → LUMO transition is a π → π excitation localized within the central N–C2–C3–C4–C5–N unit (for atom numbering see Fig. 3), with good overlap between the initial and final orbitals. This explains the larger intensity of this band as compared to the CT transition of the ring-open compounds.

In order to quantify the possibly destructive role of TICT states, which may prevent photochemical switching of compounds **1a–3a** to **1b–3b**, we optimized geometries in the first excited state of the open isomers (**1a–4a**) in the gas-phase with the B3LYP and CAM-B3LYP functionals and in acetonitrile with CAM-B3LYP. Only $S_1$ states are considered despite that excitation of the molecules with UV-light may lead to higher excited states. Nevertheless, due to internal conversion these have short lifetimes. To characterize the $S_0$ and $S_1$ states the twisting angles ω (C1,C2,C3,C4) and ω′ (C3,C4,C5,C6) of the two thiazole rings relative to the central maleimide/cyclopentene ring are compared (Table 2). Here, C1–C6 refer to labels of atoms involved in the respective dihedrals (see Fig. 3, upper left). The twisting angles are indicators of whether a TICT state is formed or not. The values in the table refer to ground and first excited singlet state of compounds **1a–4a**, for CAM-B3LYP (gas-phase) and CAM-B3LYP (acetonitrile).

First of all, we note that all dihedrals in the ground state $S_0$ are around 50°, reflecting the geometry shown in Fig. 3 (for **1a** and **4a**). A stable minimum on the first excited state surface $S_1$ could not be found for **4a** in any case. Instead, these calculations converge towards a conical intersection, which exhibits closer interatomic distances between the carbon atoms involved in ring formation. Therefore, no TICT state is formed in the $S_1$ state of **4a**, and an optical excitation should provide a reasonable quantum yield for formation of **4b** instead. In contrast, TD-CAM-B3LYP calculations in the gas-phase show a twisting of **3a** towards $\omega = 72°$. This is indicative of the formation of the TICT state, which can inhibit ring closure. On the other hand, optimizations of **1a** and **2a** in $S_1$ states approach again a conical intersection, *i.e.*, one would expect reactivity towards **1b** and **2b** in this case, or towards another photoproduct. TD-CAM-B3LYP/PCM calculations in acetonitrile provide stable structures of **1a** and **3a** in the $S_1$ excited state with twisted geometries. In these cases, however, the TICT effect appears less pronounced. Still, the ring closure will probably be hindered since a conical intersection cannot be reached easily. By contrast, for compounds **2** and **4**, optimizations lead into a conical intersection again, which may cause ring closure.

Based on these results, we conclude that **4a** has a tendency to react towards **4b** independent of method and solvent. For compounds **1a–3a** the situation is less clear. In several cases we find stable excited state structures, some of them clearly corresponding to twisted (TICT) geometries. The stable structures suggest trapped, unreactive species after photoexcitation.

From another point of view the observed photochemical switching behaviour can be rationalized qualitatively on the basis of (Kohn–Sham) frontier orbitals, which are shown exemplarily for compounds **1a** and **4a** in Fig. 3. The frontier orbitals of **2a** and **3a** are similar to those of **1a** (see Fig. S8 in the ESI†). According to the Woodward–Hoffmann rules for pericyclic reactions,[24] the LUMO of an ideal hexatriene system dominates its photoreaction, which proceeds in a conrotatory fashion as the sign of the corresponding orbital is opposite at C1 and C6. In **4a**, the computed orbitals have the same overall topology as for an ideal 6-electron π-system according to Fig. 3, right. In particular, a conrotatory ring closure is favored after photoexcitation to the $S_1$ state. This leads to a product **4b** with two methyl groups at the formed, six-membered ring in energetically favorable *trans* orientation. Thus, **4a** is expected to photoreact by orbital symmetry according to the Woodward–Hoffmann rules. In contrast, the frontier orbitals of **1a** (and also those of **2a** and **3a**) are different from the ideal situation. In particular the LUMO is now localized strongly at the maleimide ring (which is absent in **4a**), and only small coefficients are found at carbon atoms C1 and C6, which are supposed to form the C–C bond. As a consequence, ring closure does not occur after photoexcitation and instead, an

 This journal is © The Royal Society of Chemistry 2013

Published on 18 December 2012. Downloaded by Michigan State University on 19/01/2016 01:38:51.

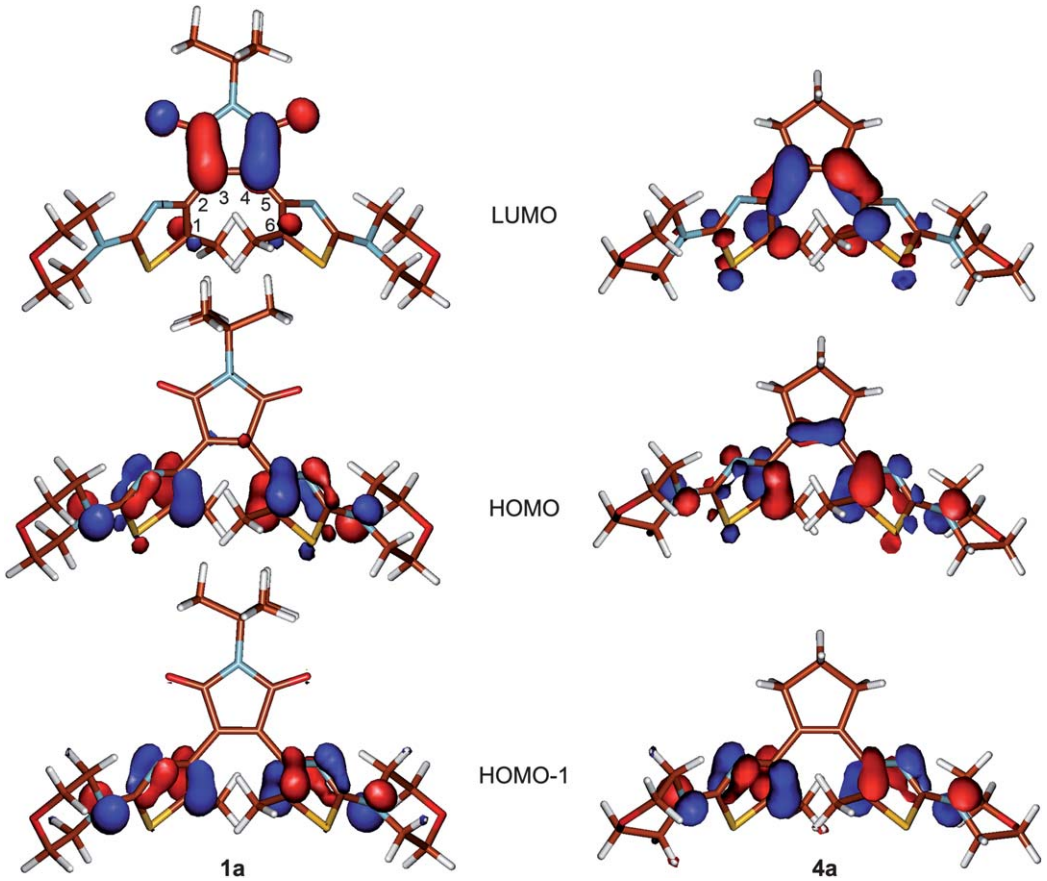


**Fig. 3** Isocontour plots of frontier orbitals for compounds **1a** and **4a** in acetonitrile, obtained on the CAM-B3LYP/PCM/6-31G* level of theory. In the upper left panel, an atom numbering for C atoms as used in the text is shown.

**Table 2** Dihedral angles $\omega$ (C1,C2,C3,C4) and $\omega'$ (C3,C4,C5,C6) (the latter in brackets if different from $\omega$) for optimized ground and first excited states $S_0$ and $S_1$ of compounds **1a–4a**, all calculated with (TD-)CAM-B3LYP/(PCM)/6-31G* for the gas-phase and in acetonitrile. In cases without an entry no stable minimum was found and a conical intersection towards ring closure was approached instead.

| | CAM-B3LYP (gas-phase) | | CAM-B3LYP (acetonitrile) | |
|---|---|---|---|---|
| Comp. | $S_0$ | $S_1$ | $S_0$ | $S_1$ |
| **1a** | 50.4 | — | 49.9 | 21.9 (22.6) |
| **2a** | 56.0 | — | 55.9 | — |
| **3a** | 49.4 (53.8) | 72.0 (33.8) | 49.8 (53.3) | 44.0 (31.1) |
| **4a** | 47.3 | — | 47.5 | — |

intramolecular charge transfer from the morpholinothiazole moiety to the maleimide ring takes place.

## Electrochemical behaviour

Cyclic voltammetry was used for the electrochemical characterization of all compounds. As irreversible oxidation processes are concerned, all reported potentials (Table 3) are peak-potentials, $E_p$, of the anodic waves and are given in reference to the ferrocene/ferrocenium ($Fc/Fc^+$) redox couple, which was used as external standard.

Upon oxidation of **1a** a single irreversible oxidation wave at a potential of 0.57 V is observed, which is associated with a charge transfer of 2 electrons per molecule (Fig. 4a). As the parent 5-methyl-2-morpholinothiazole **6** is oxidized at a very similar potential of 0.52 V, it can be assumed that the maleimide bridge has only minor influence on the oxidation potential of **1a** and thus the electron transfer originates from both electron-rich morpholinothiazole moieties. During the return scan the stepwise reduction of a new species can be observed at potentials of 0.26 V and 0.09 V corresponding to two one-electron processes. When a second scan-cycle is performed, reversible oxidation

**Table 3** Oxidation potentials of acetonitrile solutions of **1a/1b**, **2a/2b**, **3a/3b**, and **4a/4b** determined by cyclic voltammetry

| | $E_p$[a] [V] | |
|---|---|---|
| Comp. | Ring-open isomer | Ring-closed isomer |
| **1a/b** | 0.57 (irr.) | 0.15 (rev.); 0.32 (rev.) |
| **2a/b** | 1.14 (irr.) | 0.47 (rev.); 0.69 (rev.) |
| **3a/b** | 0.70 (qr); 1.23(irr.) | 0.30 (rev.); 0.52(rev.) |
| **4a/b** | 0.27 (irr.) | −0.29 (rev.); −0.19 (rev.) |

[a] Peak potentials are reported against ferrocene/ferrocenium redox couple as external standard; rev. = reversible, qr = quasireversible, irr. = irreversible.

Published on 18 December 2012. Downloaded by Michigan State University on 19/01/2016 01:38:51.

waves arise at 0.15 V and 0.32 V (Fig. 4a, inset). In analogy to the known behaviour of dithienylethenes this observation can be explained by a fast thermal reaction of oxidized **1a** to its ring-closed analogue that is subsequently reduced in two steps to **1b**, which possesses significantly lower oxidation potentials due to its conjugated structure. A charge of 2 C per mole is required during oxidation to fully convert the ring-open isomer to its ring-closed analogue. In fact, **1b** could be isolated by oxidation of the ring-open isomer on a preparative scale using two equivalents of ceric ammonium nitrate as oxidant and subsequent reduction with ascorbic acid. The structure was confirmed *via* NMR-spectroscopy and MS and its isomerization to the ring-open isomer is observed upon irradiation with 436 nm light (*vide supra*).

The oxidative ring-closure of **1a** was also followed using spectroelectrochemistry (Fig. S4 in the ESI†). While increasing the potential, the formation of an absorption band centred at 360 nm characteristic for the dicationic ring-closed isomer $\mathbf{1b}^{++}$ can be observed. During the following reduction a bathochromically shiftet absorption band around 550–750 nm evolves, indicating the presence of the monoradical cation $\mathbf{1b}^{+\cdot}$. Upon further reduction of the potential this band diminishes again and the characteristic absorption spectrum of **1b** can be observed.

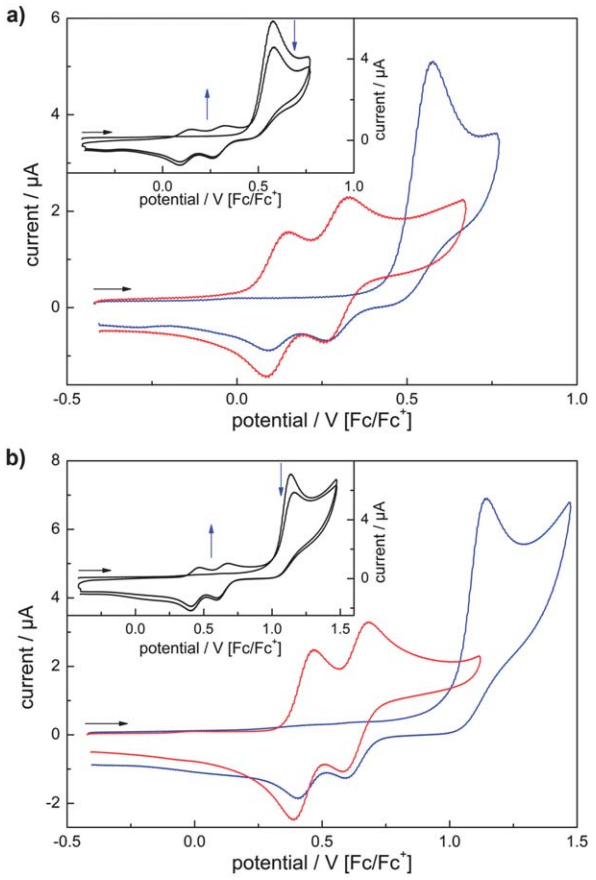


**Fig. 4** Cyclic voltammograms of the isolated ring-open isomer (blue) and ring-closed isomer (red) of (a) **1a/1b** and (b) **2a/2b** in acetonitrile ($c = 1 \times 10^{-3}$ M). Insets show two oxidative cycles consecutively performed on the respective ring-open isomer.

To test the potential of **1a** as a switch with orthogonal stimuli it was subjected to several switching cycles consisting of electrochemical oxidation/reduction of an acetonitrile solution of **1a** in a divided H-cell and subsequent irradiation of the cell with visible light ($\lambda_{irr} > 430$ nm). During this process UPLC-traces as well as UV/vis-spectra of small samples of the reaction mixture were recorded (Fig. 5). After the initial oxidation/reduction step an absorption band in the visible region corresponding to the ring-closed isomer appeared. UPLC of the reaction mixture indicated a conversion of 51% to the ring-closed isomer **1b**, but showed as well the presence of 32% of a second product **1c** (Fig. 5a). Upon irradiation with visible light ring-opening of **1b** was induced, but the initial UV-spectrum of **1a** could not be restored completely due to the photoinactivity of **1c**. Upon two more switching cycles the compound was almost completely converted to the by-product, indicated by the loss in absorbance in the visible region and by UPLC. To isolate the by-product an acetonitrile solution of **1a** was subjected to electrochemical oxidation and was subsequently stirred for 2 h at room temperature. During this time the oxidized species almost quantitatively converted to **1c**, which was then precipitated in water. Analysis of a low quality X-ray crystal structure of this material recrystallized from chloroform suggests an ionic nature for **1c** (Fig. 5c). A possible mechanism for its formation is depicted in Scheme 4: in the ring-closed dicationic state $\mathbf{1b}^{++}$, which is formed upon oxidation of **1a**, one of the thiazole methyl groups loses one proton and a subsequent nucleophilic attack of the neighboring thiazole nitrogen leads to the formation of a 7-membered ring. This assignment is supported by high resolution mass spectrometry proving the loss of one proton. Additionally, NMR-spectroscopy of the rearranged product clearly indicates the presence of two different morpholinothiazole moieties and shows a new $CH_2$ group as a broad signal at room-temperature. At lower temperatures this signal splits into two doublets showing the restricted conformational flexibility of the 7-membered ring (see Fig. S5 in the ESI†).

In order to increase the fatigue resistance of the overall switching cycle it was investigated if a substitution of the methyl groups in **1a** by trifluoromethyl groups would stabilize the dicationic species by preventing its deprotonation. In fact, the ring-open isomer **2a**, possessing trifluoromethyl groups on both thiazole rings, shows an oxidation wave centred at a peak potential of 1.14 V (Fig. 4b). Compared to **1a** this is a relatively large shift by 570 mV to higher potentials proving the strongly electron-withdrawing nature of the $CF_3$-groups. Nevertheless, the two-electron oxidation of **2a** results as well in ring closing to **2b** as can be seen from the presence of two new reversible oxidation waves in a second scan cycle. These oxidation waves show a significantly smaller shift to higher potentials of 320 mV when compared to **1b**. This is due to the formation of a quaternary carbon at the 5- and 5′-position of the thiazole moieties during the cyclization separating the $CF_3$-groups from the π-system.

When **2a** is subjected to repeated electrochemical ring-closure and photochemical ring-opening a clearly enhanced performance of the reported system can be observed.

 This journal is © The Royal Society of Chemistry 2013

Published on 18 December 2012. Downloaded by Michigan State University on 19/01/2016 01:38:51.

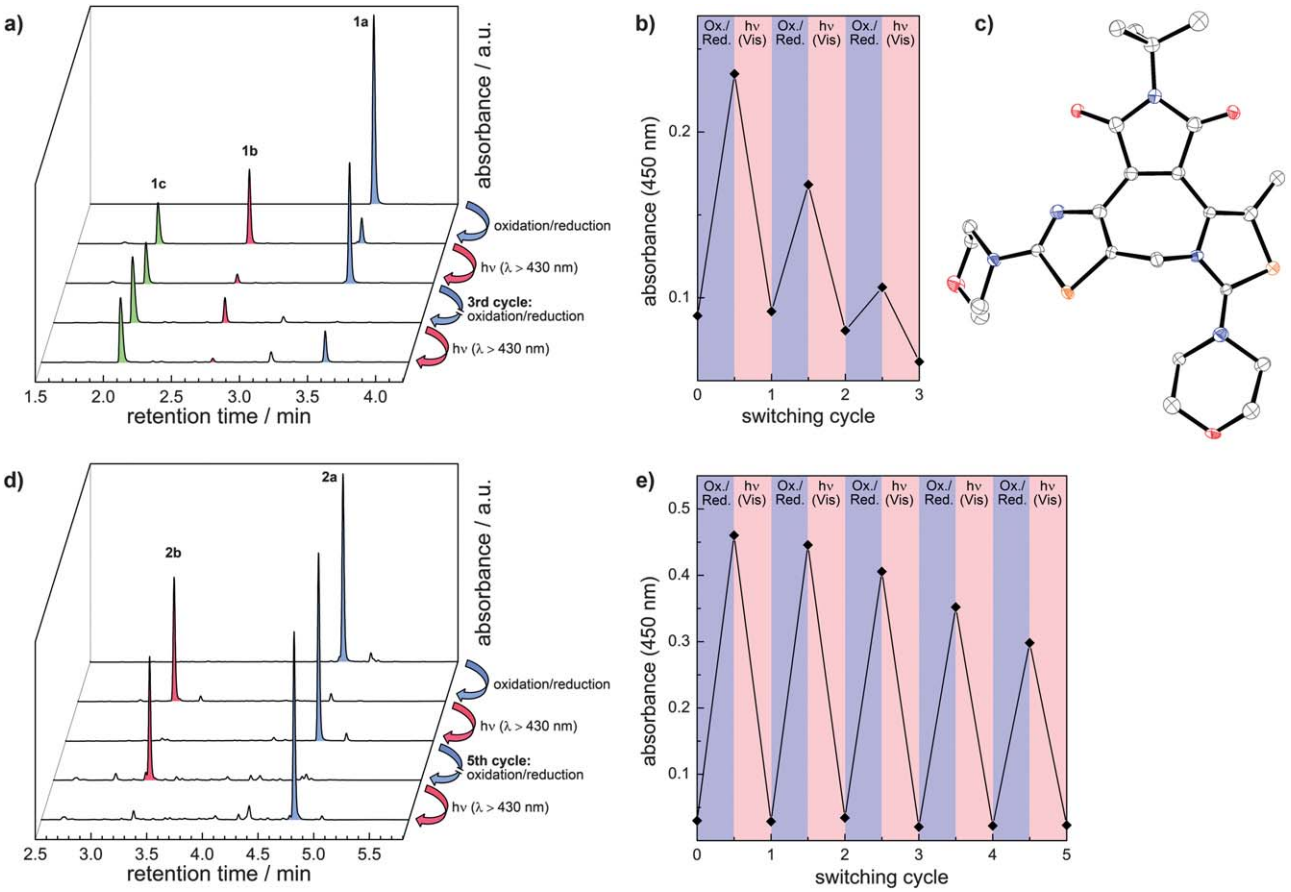


**Fig. 5** (a) UPLC-traces and (b) absorbance in the visible region of the reaction mixture recorded during repeated electrochemical ring-closure and photochemical ring-opening of **1a** in acetonitrile / 0.1 M $Bu_4NPF_6$; (c) X-ray crystal structure of low quality crystals of by-product **1c** (ORTEP-drawing, 50% probability thermal ellipsoids, hydrogen atoms and $ClO_4^-$ anion were omitted for clarity); (d) UPLC-traces and (e) absorbance in the visible region of the reaction mixture recorded during repeated electrochemical ring-closure and photochemical ring-opening of **2a** in acetonitrile / 0.1 M $Bu_4NPF_6$.

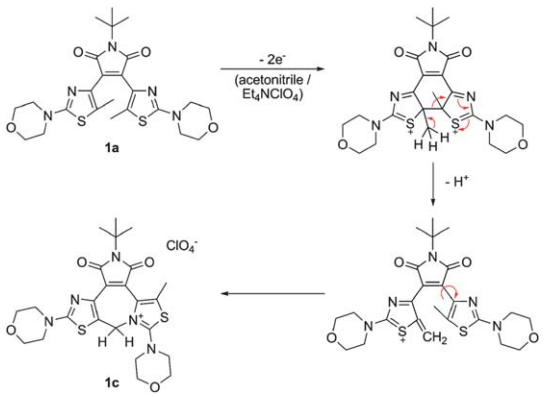


**Scheme 4** Proposed mechanism for the formation of **1c**.

UV/vis-spectra measured from small samples of the reaction mixture show the reversible formation of the absorption bands in the visible range corresponding to the ring-closed isomer (Fig. 5e). UPLC traces obtained during this experiment show almost quantitative conversion to **2b** after each oxidation/reduction step (Fig. 5d). Subsequent irradiation with visible light leads to complete cycloreversion to **2a**. There is no indication for the formation of a by-product. Nevertheless, due to diffusion of the compound into the cathode compartment of the divided electrochemical cell and due to unspecific degradation processes of the intermediate radical cationic species a continuous loss in the visible absorbance is observed during five switching cycles. This points to a general drawback of the electrochemical setup that has to be addressed in any future application; however, it does not constitute an intrinsic limitation of the molecular system.

While for the symmetrically substituted compounds **1a** and **2a** an irreversible two-electron oxidation that leads to thermal ring closure is observed in CV, the behaviour of the nonsymmetrical derivative **3a** is slightly different. Here, the cyclic voltammogram (Fig. 6) shows two well separated one-electron oxidation waves. Based on the observed oxidation potentials for compounds **1a** and **2a** the wave at 0.70 V can be assigned to the oxidation of the morpholinothiazole moiety bearing the $CH_3$-group while the wave at 1.23 V corresponds to the morpholinothiazole bearing the $CF_3$-group. The origin of the small shoulder at a potential of 1.05 V is currently unknown. Again, the total oxidative process is irreversible yielding the ring-closed species, indicated by two new oxidative waves arising at 0.42 V and 0.24 V in the second scan cycle. Most importantly, if only

Published on 18 December 2012. Downloaded by Michigan State University on 19/01/2016 01:38:51.

the morpholinothiazole bearing a $CH_3$-group is oxidized and the return point of the potential scan is set before the second oxidation takes place, the observed anodic wave has a quasi-reversible character. At a scan rate of 1 V $s^{-1}$ the first oxidation step is reversible indicated by a corresponding cathodic wave on the return scan, while at lower scan rates the formed radical cation undergoes a consecutive reaction (see Fig. S3 in the ESI†). Nevertheless, the product of this relatively slow reaction cannot be identified and is *not* identical with the ring-closed isomer, which only forms after extraction of the second electron from the ring-open species. Note that the introduction of only one $CF_3$-group into the morpholinothiazole–maleimide architecture does not improve the fatigue resistance of the electrochemical switching process. During the oxidative cyclization of **3a** a by-product similar to that described earlier for **1a** could be observed in UPLC/MS-measurements.

## Mechanistic considerations

The mechanistic pathway for the oxidative ring-closure or ring-opening of diarylethenes is still under discussion. Recently both radical cationic intermediates[7c,13,25] as well as dicationic intermediates[8d,26] were identified to be the species undergoing the thermal isomerization reaction between the ring-open and the ring-closed isomer. For the oxidative cyclization reaction studied in *this* work both possibilities would experimentally lead to similiar observations: for a reaction through a monocationic state one would postulate an ECE-mechanism[27] consisting of an initial electron transfer from the ring-open isomer giving the radical cation, which subsequently undergoes fast cyclization. As the resulting ring-closed isomer possesses a lower oxidation potential, a second electron is then transferred immediately to the electrode resulting in the ring-closed dicationic species. Nevertheless, an EEC-mechanism could also be possible: supposing both morpholinothiazole moieties of the ring-open isomer are electronically decoupled by twisting of the ring-planes and cross-conjugation through the bridge, they can be seen as independent redox centres that in case of a symmetrical molecule get oxidized simultaneously or at least at very similar potentials.[28] Thus a diradical dication of the open form is built that cyclizes to the dicationic ring-closed isomer. In both cases, cyclic voltammetry shows an irreversible two-electron oxidation of the ring-open isomer.

A first hint that directs towards the latter EEC-mechanism is the lack of any bathochromic absorbance during the spectroelectrochemical investigation of the oxidation of **1a** (Fig. S4 of the ESI†), which would be characteristic for an intermediate monoradical cationic species either in the ring-open or in the ring-closed form. A similar observation has recently been made for a related dithienylethene possessing amine redox centres attached directly to the thiophene rings.[26a]

To further prove this assumption of an operating EEC-mechanism a nonsymmetrically substituted derivative is necessary in order to achieve a maximum difference in the oxidation potentials of both aryl units. The reported derivative **3a** was synthesized specifically for this task. The introduction of the $CF_3$-unit did not alter the properties of the morpholinothiazole as a redox centre apart from a significant shift of its oxidation potential by 570 mV.[29] In fact, from cyclic voltammetry of **3a** as described above (Fig. 6) it is clear that the first electron transfer from the molecule has a quasireversible nature and does not lead to a chemical reaction at high scan rates. Therefore, a stepwise *double* ionization to a dicationic species has to take place in order to induce the ring-closure and thus we conclude that the oxidative cyclization of **3a** follows an EEC-mechanism (Scheme 5).

Calculations were also performed to rationalize the electrochemical behaviour of compounds **1–4** and to gain more detailed insight into the isomerization mechanism. For this purpose, we considered different ionized species and different electronic configurations. First, monocations with doublet spin multiplicity (henceforth $^{D}A^{+}$) were treated with the unrestricted B3LYP (UB3LYP) method. Second, we studied various dications. Closed-shell dications with singlet multiplicity ($^{S}A^{2+}$) were treated with restricted B3LYP (RB3LYP) and dications with triplet multiplicity ($^{T}A^{2+}$) were treated with UB3LYP. Finally, also open-shell dications with singlet multiplicity were treated with UB3LYP, using the broken symmetry approach ($^{SU}A^{2+}$). The (broken symmetry) UB3LYP calculations for the dication serve

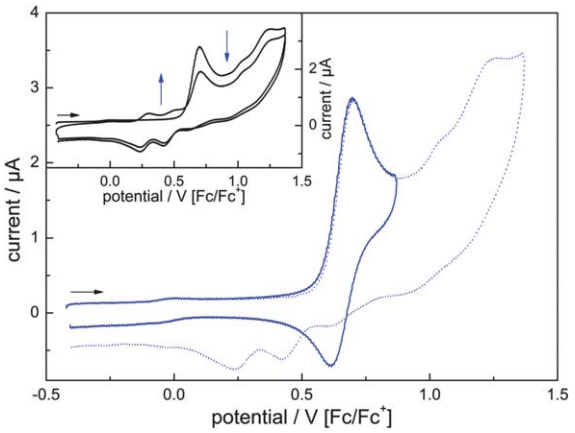


**Fig. 6** Cyclic voltammetry of **3a** in acetonitrile ($c = 1 \times 10^{-3}$ M, scan rate 1 V $s^{-1}$) using a return potential at 0.87 V (solid line) and at 1.37 V (dotted line), respectively. Inset shows two full oxidative cycles consecutively performed on the ring-open isomer.

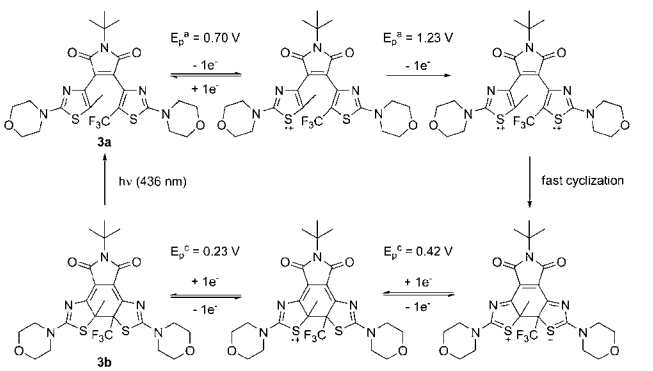


**Scheme 5** EEC-mechanism for the oxidative ring-closure of **3a**.


This journal is © The Royal Society of Chemistry 2013

Published on 18 December 2012. Downloaded by Michigan State University on 19/01/2016 01:38:51.

as models for triplet and singlet biradicals, respectively,[30] within a single-determinant formalism. When applied to the open forms, the singlet biradical is characterized by two unpaired α and β electrons which are well separated in space, localized on either the left or the right morpholino thiazole moiety, as shown in Fig. S9 of the ESI.† Similarly, the two excess α spins of the triplet dication are also localized at these units as shown there. Since only ground states (and no long-range charge transfer excitations) were considered here, the B3LYP method was used as it is reliable in this case. Again, PCM embedding was used to model solvents.

We first performed ΔSCF calculations with reoptimized geometries for ions giving *adiabatic* ionization potentials

$$\mathrm{IP}(\mathrm{A}^{n+} \rightarrow \mathrm{A}^{m+}) = E(\mathrm{A}^{m+}) - E(\mathrm{A}^{n+}), \quad (1)$$

where $n$ and $m$ denote the positive charge ($n,m = 0$, 1, or 2) of the molecule. Note that $\mathrm{IP}(\mathrm{A}^0 \rightarrow \mathrm{A}^{2+}) = \mathrm{IP}(\mathrm{A}^0 \rightarrow \mathrm{A}^{1+}) + \mathrm{IP}(\mathrm{A}^{1+} \rightarrow \mathrm{A}^{2+})$. The adiabatic IPs for the different switches exposed to a PCM (acetonitrile) field were calculated (Table 4). Furthermore, the corresponding gas-phase values, as well as ΔSCF energy differences for *vertical* ionizations, $\mathrm{IP}^{\mathrm{v}}(\mathrm{A}^{n+} \rightarrow \mathrm{A}^{m+})$, *i.e.* without reoptimization of ion geometries, were determined (see Section 10 of the ESI†).

First of all we note that the calculated IPs (Table 4) reveal very nicely the trends observed experimentally for the impact of substitution on the electrochemical behaviour of compounds **1–4**. For example, when going from bis-$CH_3$-substituted **1a** to bis-$CF_3$-substituted **2a** the experimental oxidation potential increases by 0.57 V, while theory predicts a shift of 0.54 eV for the first ionization potential $\mathrm{IP}(\mathrm{A}^0 \rightarrow \mathrm{A}^{1+})$. Furthermore, the significantly lower ionization potentials for the ring-closed species **1b–4b** are reproduced very well by the quantum mechanical calculations: the first ionization potentials $\mathrm{IP}(\mathrm{A}^0 \rightarrow \mathrm{A}^{1+})$ are lower by between 0.39 eV (for **1**) and 0.68 eV (for **4**) than the corresponding values for the ring-open species, while experimentally potential shifts between 0.42 V (for **1**) and 0.56 V (for **4**) are found. Concerning doubly ionized species, from the $\mathrm{IP}(\mathrm{A}^0 \rightarrow \mathrm{A}^{2+})$-values it can be seen that for the ring-open isomers **1a–4a** the singlet biradical ($^{\mathrm{SU}}\mathrm{A}^{2+}$) is slightly more stable or at least equally stable as compared to the triplet biradical ($^{\mathrm{T}}\mathrm{A}^{2+}$), and always more stable than the closed-shell singlet ($^{\mathrm{S}}\mathrm{A}^{2+}$). For the ring-closed forms **1b–4b** no broken symmetry solution can be found for the singlet state, *i.e.* the UB3LYP and RB3LYP calculations give the same result with only paired electrons. For the closed form the triplet dication is always significantly less stable than the singlet.

Interestingly, for the ring-closed compounds **1b–4b** the experimentally observed potential splitting $\Delta E_{\mathrm{p}}$, defined as the difference between the first and the second oxidation potential $E_{\mathrm{p},2} - E_{\mathrm{p},1}$, is significantly overestimated by the quantum mechanical calculations. While experimental $\Delta E_{\mathrm{p}}$ vary between 0.22 V (for **2b**) and 0.10 V (for **4b**) the according differences between the theoretical first and second ionization potentials ΔIP $= \mathrm{IP}(\mathrm{A}^{1+} \rightarrow \mathrm{A}^{2+}) - \mathrm{IP}(\mathrm{A}^0 \rightarrow \mathrm{A}^{1+})$ are in the range of 0.79 eV (for **2b**) and 0.72 eV (for **4b**), referring to the formation of the most stable $^{\mathrm{SU}}\mathrm{A}^{2+}$ dications. The ΔIP-values for gas-phase calculations (see Table S5 in the ESI†) are 4–5 times higher (3.43–3.56 eV) showing the extraordinary role of the solvent for the stabilization of the charge of a dicationic species.[31] Note that it has been described earlier that DFT-calculations on this level of theory using PCM to consider solvent effects underestimate this stabilization energy and thus, the resulting compression of potential splitting observed in the experiment is not reproduced accurately.[32]

As described above, the ring-open compounds, except for the nonsymmetrical derivative **3a**, do not show any potential splitting in their two electron oxidation waves. This behaviour can be rationalized in terms of electronic decoupling of the two identical electrophores in the ring-open form. Thus, only electrostatic effects play a role for the additional energy required for extracting the second electron from the molecule. For localized charges this may be compensated by the solvent and to a lesser extent by the supporting electrolyte leading to a situation where $E_{\mathrm{p},2} \leq E_{\mathrm{p},1}$, which allows for the simultaneous oxidation of both electrophores *via* a concerted electron transfer or a disproportionation mechanism.[28] This is revealed as well in the theoretical ΔIP-values for the ring-open forms (0.35–0.68 eV) that are considerably smaller than the corresponding values for the ring-closed forms. Nevertheless, they fail to reproduce the experimentally observed complete compression of potential splitting for compounds **1a**, **2a**, and **4a**. However, note that the above arguments are valid only for strictly reversible oxidation processes. As in our experiment the chemical reaction subsequent to the second oxidation step is very fast, the equilibrium may be shifted to the dicationic product despite the absence of an exergonic second electron transfer.

The calculations also nicely explain the reactivity of dications towards ring closure. For this purpose, we determined transition states for the ring closure reaction of neutral as well as charged species. For this purpose the so-called QST3 method,[33] again in conjunction with B3LYP/PCM/6-31G*, was used. There are in principle at least two possible reaction products, arising from either the conrotatory or the disrotatory pathway, where the two ligands at C1 and C6 (–$CH_3$ or –$CF_3$) end up in a *trans* or in a *cis* orientation, respectively. Therefore, one also expects at least two transition states. The energies of the conrotatory products (**b**) and corresponding transition states (‡) were calculated relative to the reactants (open, **a**) (Table 5). Table 5 further contains an

**Table 4** Adiabatic ionization potentials $\mathrm{IP}(\mathrm{A}^{n+} \rightarrow \mathrm{A}^{m+})$ in eV calculated as energy differences between neutral ($\mathrm{A}^0$) and reoptimized ions ($\mathrm{A}^+$ and $\mathrm{A}^{2+}$), obtained on the B3LYP/PCM(acetonitrile)/6-31G* level of theory. For the dication three different configurations were used (see text).

| | $\mathrm{IP}(\mathrm{A}^0 \rightarrow \mathrm{A}^+)$ | $\mathrm{IP}(\mathrm{A}^0 \rightarrow \mathrm{A}^{2+})$ | | | $\mathrm{IP}(\mathrm{A}^+ \rightarrow \mathrm{A}^{2+})$ | | |
|---|---|---|---|---|---|---|---|
| | $^{\mathrm{D}}\mathrm{A}^+$ | $^{\mathrm{S}}\mathrm{A}^{2+}$ | $^{\mathrm{SU}}\mathrm{A}^{2+}$ | $^{\mathrm{T}}\mathrm{A}^{2+}$ | $^{\mathrm{S}}\mathrm{A}^{2+}$ | $^{\mathrm{SU}}\mathrm{A}^{2+}$ | $^{\mathrm{T}}\mathrm{A}^{2+}$ |
| **1a** | 5.02 | 10.82 | 10.52 | 10.54 | 5.80 | 5.50 | 5.52 |
| **1b** | 4.63 | 10.00 | 10.00 | 11.53 | 5.37 | 5.37 | 6.90 |
| **2a** | 5.56 | 11.98 | 11.47 | 11.47 | 6.42 | 5.91 | 5.91 |
| **2b** | 4.90 | 10.59 | 10.59 | 11.98 | 5.69 | 5.69 | 7.08 |
| **3a** | 5.16 | 11.34 | 10.99 | 11.00 | 6.18 | 5.83 | 5.84 |
| **3b** | 4.76 | 10.30 | 10.30 | 11.74 | 5.54 | 5.54 | 6.98 |
| **4a** | 4.71 | Instable | 10.10 | 10.16 | — | 5.39 | 5.45 |
| **4b** | 4.03 | 8.78 | 8.78 | 10.53 | 8.78 | 4.75 | 6.50 |

Published on 18 December 2012. Downloaded by Michigan State University on 19/01/2016 01:38:51.

entry $\Delta E_g$ for each species, which is the maximal possible energy, which can be gained in the ionized state by geometry relaxation. The latter is given as the reorganization energy

$$\Delta E_g = \mathrm{IP}^v(A^{n+} \rightarrow A^{m+}) - \mathrm{IP}(A^{n+} \rightarrow A^{m+}). \quad (2)$$

This quantity is calculated for the open (**a**) species only. If $\Delta E_g > E_{act} = E((A^{m+})^{\ddagger}) - E(A^{m+})$ at least a purely energetic criterion to overcome the activation energy $E_{act}$ for ring closure is fulfilled. Of course, this does not necessarily imply that the reaction actually takes place.

From the results it is apparent that most of the ring closure reactions are exergonic. Exceptions are compound **4** in its neutral form, as well as all triplet dications. Singly charged cations, and even more so singlet dications give large, negative reaction energies up to −1.47 eV (for the singlet dication $^{S}$**2a**$^{2+}$).

Similarly, there are also large variations in activation energies for ring closure. For neutral molecules we find high barriers of around 2 eV for **1a–3a**, and an even higher barrier of 2.61 eV for compound **4a**, reflecting the fact that the **a** → **b** reactions of neutral species are all thermally forbidden by the Woodward–Hoffmann rules (*vide infra*). For the monocations, we find activation energies between 0.77 eV (for $^{D}$**3a**$^{+}$) to 0.92 eV (for $^{D}$**4a**$^{+}$). For a purely thermal reaction these are high barriers as well, suggesting small reaction rates. The maximal energy gain $\Delta E_g$ is significantly smaller than the activation energies, making it very unlikely that the molecules can overcome this ground-state barrier.

The smallest barriers are found for singlet dications ($^{S}A^{2+}$). The classical barriers, *i.e.* without vibrational corrections, are close to zero for the singlet closed-shell dications $^{S}$**1a**$^{2+}$ to $^{S}$**3a**$^{2+}$. For the $^{S}$**4a**$^{2+}$ singlet closed-shell dication, no stable isomer and transition state could be found. Due to the considerable energy gained during relaxation, these rather small barriers should readily be overcome, even at lower temperatures. For singlet biradical dications ($^{SU}A^{2+}$) the activation energies towards ring closure are between 0.05 eV (for $^{SU}$**4a**$^{2+}$) and 0.52 eV (for $^{SU}$**2a**$^{2+}$). Nevertheless, also in this case reorganization energies $\Delta E_g$ are larger than activation energies, suggesting high reaction rates again. Since the ring-open isomers treated as singlet biradical dications ($^{SU}A^{2+}$) show the lowest total energy as demonstrated above, we expect, on this level of theory, that the electrochemical ring closure leading to a conrotatory (*trans*) product is dominated by a reaction on the biradical singlet potential energy surface of the dication. Reactions of the dication on the triplet surface are not favored. The monocationic surface will also play only a minor role. For the thermal cyclization reaction of compound **3a** these findings are summarized in Fig. 7.

For compound **3** we also considered a disrotatory pathway leading to the *cis*-product (see Table S8 of the ESI†). We note that the energies for ring-closed species **3b**(dis) are always less favorable in comparison to the respective conrotatory products. In most cases the reaction is endergonic. The corresponding activation energies $E_{act}$(dis) are larger than the $E_{act}$(con) values for all cations, but smaller for the neutral species. Thus, for neutral species a thermal reaction would proceed faster (albeit still slow) along the disrotatory pathway, in agreement with Woodward–Hoffmann rules. In general, however, the disrotatory pathway is neither kinetically nor thermodynamically attractive in comparison to the conrotatory one.

Thermally induced neutral and monocationic ground state reactions are dominated by the HOMO. From Fig. 3 one can see that for the compounds under discussion one finds that the HOMO, at least as far as the carbon atoms C1 and C6 are concerned, have a phase similar to what one expects from ideal hexatriene, *i.e.*, the phase on C1 and C6 are of the same sign. As a consequence, the ring closure would have to proceed in a disrotatory manner. Still, this process is associated with large barriers due to the presence of the two additional $CH_3$- or $CF_3$-groups at C1 and C6, while the barrier for the conrotatory pathway is even larger, in agreement with the Woodward–Hoffmann rules. In the end, a thermal ring-closure reaction is unfavorable for neutral molecules and monocations. For the dications reacting thermally, one expects a prominent role for HOMO-1. From Fig. 3 we note that both for **1a** and **4a** the coefficients at C1 and C6 in this orbital are large and have opposite sign, in agreement with what one expects for an ideal 6-electron conjugated π-system. Therefore, a conrotatory pathway leading to the *trans* product should be easily accessible, which explains the shallow barriers observed for the singlet dications $^{S}A^{2+}$ according to Table 5. Of course, this analysis holds strictly for restricted orbitals only, which are shown in Fig. 3. For the unrestricted (UB3LYP) orbitals used for the open-shell singlet and triplet dications the situation is more complicated. This leads eventually to unfavorable pathways for the triplet, and to finite, but not too large, barriers for the biradical singlet state. Due to the favorable reaction energies, the biradical singlet $^{SU}A^{2+}$ appears to be the most probable reaction channel for electrochemical ring closure as outlined above.

**Table 5** Energies (in eV) relative to open forms (**a**) for compounds **1–4** according to B3LYP/PCM(acetonitrile)/6-31G* calculations. The $\Delta E_g$ values are maximum energy gains of ionic ring-open species as defined in eqn (2). Product and transition state energies refer to the conrotatory pathway for the cyclization reaction.

| | Neutral | $^{D}A^{+}$ | $^{S}A^{2+}$ | $^{SU}A^{2+}$ | $^{T}A^{2+}$ |
|---|---|---|---|---|---|
| **1a** | 0.00 | 0.00 | 0.00 | 0.00 | 0.00 |
| **1b** | −0.29 | −0.68 | −1.11 | −0.81 | 0.70 |
| **1**$^{\ddagger}$ | 2.09 | 0.86 | 0.01 | 0.30 | 1.80 |
| $\Delta E_g$ | | 0.25 | 0.84 | 0.66 | 0.66 |
| **2a** | 0.00 | 0.00 | 0.00 | 0.00 | 0.00 |
| **2b** | −0.08 | −0.74 | −1.47 | −0.96 | 0.43 |
| **2**$^{\ddagger}$ | 2.10 | 0.77 | 0.01 | 0.52 | 1.62 |
| $\Delta E_g$ | | 0.21 | 0.67 | 0.56 | 0.56 |
| **3a** | 0.00 | 0.00 | 0.00 | 0.00 | 0.00 |
| **3b** | −0.22 | −0.61 | −1.25 | −0.91 | 0.52 |
| **3**$^{\ddagger}$ | 2.02 | 0.92 | 0.01 | 0.35 | 1.68 |
| $\Delta E_g$ | | 0.29 | 0.77 | 0.62 | 0.62 |
| **4a** | 0.00 | 0.00 | Instable | 0.00 | 0.00 |
| **4b** | 0.07 | −0.63 | — | −1.28 | 0.41 |
| **4**$^{\ddagger}$ | 2.61 | 0.82 | — | 0.05 | 1.80 |
| $\Delta E_g$ | | 0.18 | — | 0.44 | 0.42 |


This journal is © The Royal Society of Chemistry 2013

Published on 18 December 2012. Downloaded by Michigan State University on 19/01/2016 01:38:51.

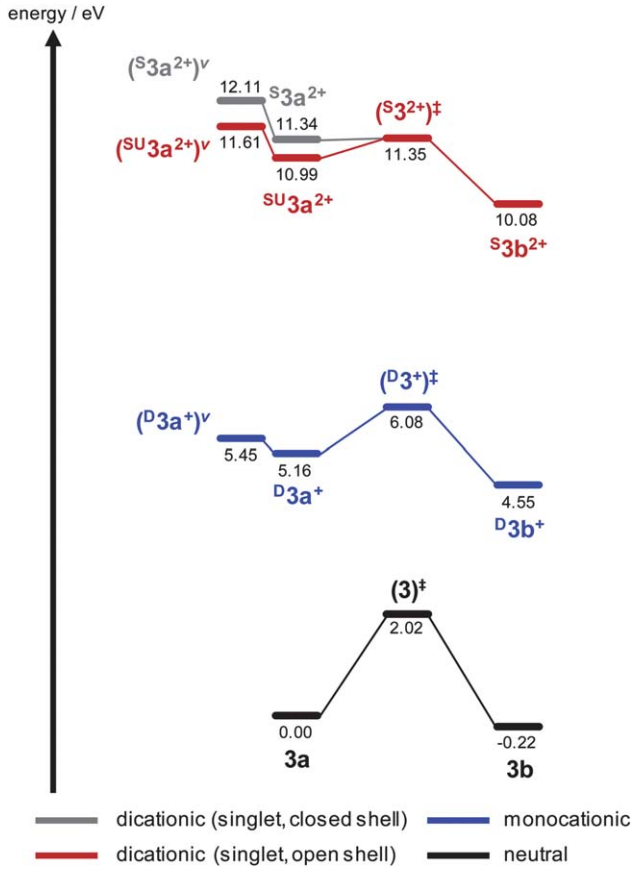


**Fig. 7** Energy profile for the thermal cyclization reaction of **3a** in its neutral, monocationic, and dicationic forms. Energies are in eV, relative to **3a**.

## Conclusions

We have described the first dithiazolylethene derivative, which undergoes an electrochemically driven conversion from the ring-open to its ring-closed form. While oxidative ring-closure is facilitated by the presence of the terminal electron-donating morpholino substituent, photocyclization is inhibited due to an intramolecular charge transfer interaction. Since cycloreversion can only be affected by light (and not by electrochemical means), the system described herein can be addressed by two different "orthogonal" stimuli. Optimization of the chemical structure by introduction of trifluoromethyl groups into either one or both reactive terminal hexatrienyl positions (C1 and/or C6) not only allowed for elucidation of the mechanism of oxidative cyclization *via* the dicationic intermediate, as independently shown by DFT calculations, but provides access to fatigue resistant versions of these unique "orthogonal" photo-electro-chromes. These compounds should be of interest for designing multifunctional devices with logic functions responding to photons and electrons as discrete inputs. Perhaps even more importantly, such systems point to a potential way of using switches not as elements of remote spatiotemporal control over a given function ("trigger"), but they may be used to convert light into electrical energy *via* photon-driven generation of meta-stable states with sufficient electrochemical potential to promote chemical (redox) reactions ("drivers"). Work to exploit this and similar systems for solar energy conversion and storage is currently ongoing in our laboratories.

## Acknowledgements

The authors are grateful to Stefan Mebs (Department of Chemistry, Humboldt-Universität zu Berlin) for obtaining the Xray crystal structures of **1a** and **1c**. Generous support by the German Research Foundation (DFG *via* SFB 658, projects B8 and C2) is gratefully acknowledged. BASF AG, Bayer Industry Services, and Sasol Germany are thanked for generous donations of chemicals.

## Notes and references

1 (*a*) J. Zhang, Q. Zou and H. Tian, *Adv. Mater.*, 2012, DOI: 10.1002/adma.201201521; (*b*) D. Gust, J. Andreasson, U. Pischel, T. A. Moore and A. L. Moore, *Chem. Commun.*, 2012, **48**, 1947; (*c*) M. Natali and S. Giordani, *Chem. Soc. Rev.*, 2012, **41**, 4010; (*d*) O. S. Wenger, *Chem. Soc. Rev.*, 2012, **41**, 3772; (*e*) M. Akita, *Organometallics*, 2011, **30**, 43; (*f*) D. Bleger, Z. Yu and S. Hecht, *Chem. Commun.*, 2011, **47**, 12260; (*g*) M.-M. Russew and S. Hecht, *Adv. Mater.*, 2010, **22**, 3348; (*h*) R. S. Stoll and S. Hecht, *Angew. Chem., Int. Ed.*, 2010, **49**, 5054; (*i*) R. Klajn, J. F. Stoddart and B. A. Grzybowski, *Chem. Soc. Rev.*, 2010, **39**, 2203; (*j*) H. Tian and S. Wang, *Chem. Commun.*, 2007, 781; (*k*) F. M. Raymo and M. Tomasulo, *Chem. Soc. Rev.*, 2005, **34**, 327.

2 M. Irie, *Chem. Rev.*, 2000, **100**, 1685.

3 (*a*) R. C. Shallcross, P. Zacharias, A. Köhnen, P. O. Körner, E. Maibach and K. Meerholz, *Adv. Mater.*, 2012, DOI: 10.1002/adma.201202186; (*b*) M. Pärs, C. C. Hofmann, K. Willinger, P. Bauer, M. Thelakkat and J. Köhler, *Angew. Chem., Int. Ed.*, 2011, **50**, 11405; (*c*) J. Andréasson, U. Pischel, S. D. Straight, T. A. Moore, A. L. Moore and D. Gust, *J. Am. Chem. Soc.*, 2011, **133**, 11641; (*d*) T. Fukaminato, T. Doi, N. Tamaoki, K. Okuno, Y. Ishibashi, H. Miyasaka and M. Irie, *J. Am. Chem. Soc.*, 2011, **133**, 4984.

4 (*a*) E. Orgiu, N. Crivillers, M. Herder, L. Grubert, M. Pätzel, J. Frisch, E. Pavlica, D. T. Duong, G. Bratina, A. Salleo, N. Koch, S. Hecht and P. Samorì, *Nat. Chem.*, 2012, **4**, 675; (*b*) T. Tsujioka, T. Sasa and Y. Kakihara, *Org. Electron.*, 2012, **13**, 681; (*c*) P. Zacharias, M. C. Gather, A. Köhnen, N. Rehmann and K. Meerholz, *Angew. Chem., Int. Ed.*, 2009, **48**, 4038; (*d*) A. J. Kronemeijer, H. B. Akkerman, T. Kudernac, B. J. van Wees, B. L. Feringa, P. W. M. Blom and B. de Boer, *Adv. Mater.*, 2008, **20**, 1467.

5 (*a*) B. M. Neilson and C. W. Bielawski, *J. Am. Chem. Soc.*, 2012, **134**, 12693; (*b*) M. Morimoto, K. Murata and T. Michinobu, *Chem. Commun.*, 2011, **47**, 9819; (*c*) D. Wilson and N. R. Branda, *Angew. Chem., Int. Ed.*, 2012, **51**, 5431; (*d*) V. Lemieux, M. Spantulescu, K. Baldridge and N. Branda, *Angew. Chem., Int. Ed.*, 2008, **47**, 5034; (*e*) Z. Erno, A. M. Asadirad, V. Lemieux and N. R. Branda, *Org. Biomol. Chem.*, 2012, **10**, 2787.

Published on 18 December 2012. Downloaded by Michigan State University on 19/01/2016 01:38:51.

6 (*a*) X. Zhou, Y. Duan, S. Yan, Z. Liu, C. Zhang, L. Yao and G. Cui, *Chem. Commun.*, 2011, **47**, 6876; (*b*) M. Herder, M. Patzel, L. Grubert and S. Hecht, *Chem. Commun.*, 2011, **47**, 460; (*c*) T. Hirose, M. Irie and K. Matsuda, *Adv. Mater.*, 2008, **20**, 2137; (*d*) M. Takeshita, M. Hayashi, S. Kadota, K. H. Mohammed and T. Yamato, *Chem. Commun.*, 2005, 761; (*e*) L. N. Lucas, J. van Esch, R. M. Kellogg and B. L. Feringa, *Chem. Commun.*, 2001, 759.

7 (*a*) W. R. Browne, T. Kudernac, N. Katsonis, J. Areephong, J. Hjelm and B. L. Feringa, *J. Phys. Chem. C*, 2008, **112**, 1183; (*b*) J. Areephong, W. R. Browne, N. Katsonis and B. L. Feringa, *Chem. Commun.*, 2006, 3930; (*c*) Y. Moriyama, K. Matsuda, N. Tanifuji, S. Irie and M. Irie, *Org. Lett.*, 2005, **7**, 3315; (*d*) A. Peters and N. R. Branda, *Chem. Commun.*, 2003, 954; (*e*) A. Peters and N. R. Branda, *J. Am. Chem. Soc.*, 2003, **125**, 3404; (*f*) T. Koshido, T. Kawai and K. Yoshino, *J. Phys. Chem.*, 1995, **99**, 6110.

8 (*a*) Y.-M. Hervault, C. M. Ndiaye, L. Norel, C. Lagrost and S. Rigaut, *Org. Lett.*, 2012, **14**, 4454; (*b*) Y. Tanaka, T. Ishisaka, A. Inagaki, T. Koike, C. Lapinte and M. Akita, *Chem.–Eur. J.*, 2010, **16**, 4762; (*c*) Y. Lin, J. Yuan, M. Hu, J. Cheng, J. Yin, S. Jin and S. H. Liu, *Organometallics*, 2009, **28**, 6402; (*d*) Y. Liu, C. Lagrost, K. Costuas, N. Tchouar, H. L. Bozec and S. Rigaut, *Chem. Commun.*, 2008, 6117; (*e*) K. Motoyama, T. Koike and M. Akita, *Chem. Commun.*, 2008, 5812; (*f*) G. Guirado, C. Coudret and J.-P. Launay, *J. Phys. Chem. C*, 2007, **111**, 2770.

9 (*a*) A. Léaustic, E. Anxolabéhère-Mallart, F. Maurel, S. Midelton, R. Guillot, R. Métivier, K. Nakatani and P. Yu, *Chem.–Eur. J.*, 2011, **17**, 2246; (*b*) B. Gorodetsky, H. D. Samachetty, R. L. Donkers, M. S. Workentin and N. R. Branda, *Angew. Chem., Int. Ed.*, 2004, **43**, 2812.

10 B. Gorodetsky and N. R. Branda, *Adv. Funct. Mater.*, 2007, **17**, 786.

11 (*a*) R. Göstl, B. Kobin, L. Grubert, M. Pätzel and S. Hecht, *Chem.–Eur. J.*, 2012, DOI: 10.1002/chem.201203111; (*b*) H. Ogawa, K. Takagi, T. Ubukata, A. Okamoto, N. Yonezawa, S. Delbaere and Y. Yokoyama, *Chem. Commun.*, 2012, **48**, 11838; (*c*) S. Fukumoto, T. Nakashima and T. Kawai, *Eur. J. Org. Chem.*, 2011, 5047; (*d*) S. Fukumoto, T. Nakashima and T. Kawai, *Angew. Chem., Int. Ed.*, 2011, **50**, 1565; (*e*) K. Morinaka, T. Ubukata and Y. Yokoyama, *Org. Lett.*, 2009, **11**, 3890.

12 M. Irie, T. Lifka, K. Uchida, S. Kobatake and Y. Shindo, *Chem. Commun.*, 1999, 747.

13 (*a*) G. Guirado, C. Coudret, M. Hliwa and J.-P. Launay, *J. Phys. Chem. B*, 2005, **109**, 17445; (*b*) W. R. Browne, J. J. D. de Jong, T. Kudernac, M. Walko, L. N. Lucas, K. Uchida, J. H. van Esch and B. L. Feringa, *Chem.–Eur. J.*, 2005, **11**, 6414; (*c*) W. R. Browne, J. J. D. de Jong, T. Kudernac, M. Walko, L. N. Lucas, K. Uchida, J. H. van Esch and B. L. Feringa, *Chem.–Eur. J.*, 2005, **11**, 6430.

14 (*a*) K. Uchida, T. Ishikawa, M. Takeshita and M. Irie, *Tetrahedron*, 1998, **54**, 6627–6638; (*b*) S. Takami, S. Kobatake, T. Kawai and M. Irie, *Chem. Lett.*, 2003, **32**, 892–893.

15 F. Cottet and M. Schlosser, *Eur. J. Org. Chem.*, 2002, 327.

16 M. Ohsumi, M. Hazama, T. Fukaminato and M. Irie, *Chem. Commun.*, 2008, 3281.

17 Z. R. Grabowski, K. Rotkiewicz and W. Rettig, *Chem. Rev.*, 2003, **103**, 3899.

18 K. Morimitsu, S. Kobatake, S. Nakamura and M. Irie, *Chem. Lett.*, 2003, **32**, 858.

19 (*a*) A. D. Becke, *J. Chem. Phys.*, 1993, **98**, 5648; (*b*) R. Ditchfield, W. J. Hehre and J. A. Pople, *J. Chem. Phys.*, 1971, **54**, 724.

20 T. Yanai, D. P. Tew and N. C. Handy, *Chem. Phys. Lett.*, 2004, **393**, 51.

21 S. Miertuš, E. Scrocco and J. Tomasi, *Chem. Phys.*, 1981, **55**, 117.

22 M. E. Casida, C. Jamorski, K. C. Casida and D. R. Salahub, *J. Chem. Phys.*, 1998, **108**, 4439.

23 M. J. Frisch, G. W. Trucks, H. B. Schlegel, G. E. Scuseria, M. A. Robb, J. R. Cheeseman, G. Scalmani, V. Barone, B. Mennucci, G. A. Petersson, H. Nakatsuji, M. Caricato, X. Li, H. P. Hratchian, A. F. Izmaylov, J. Bloino, G. Zheng, J. L. Sonnenberg, M. Hada, M. Ehara, K. Toyota, R. Fukuda, J. Hasegawa, M. Ishida, T. Nakajima, Y. Honda, O. Kitao, H. Nakai, T. Vreven, J. A. Montgomery Jr, J. E. Peralta, F. Ogliaro, M. Bearpark, J. J. Heyd, E. Brothers, K. N. Kudin, V. N. Staroverov, R. Kobayashi, J. Normand, K. Raghavachari, A. Rendell, J. C. Burant, S. S. Iyengar, J. Tomasi, M. Cossi, N. Rega, J. M. Millam, M. Klene, J. E. Knox, J. B. Cross, V. Bakken, C. Adamo, J. Jaramillo, R. Gomperts, R. E. Stratmann, O. Yazyev, A. J. Austin, R. Cammi, C. Pomelli, J. W. Ochterski, R. L. Martin, K. Morokuma, V. G. Zakrzewski, G. A. Voth, P. Salvador, J. J. Dannenberg, S. Dapprich, A. D. Daniels, Ö. Farkas, J. B. Foresman, J. V. Ortiz, J. Cioslowski and D. J. Fox, *Gaussian 09 Revision A.02*, Gaussian Inc., Wallingford CT, 2009.

24 R. B. Woodward and R. Hoffmann, *J. Am. Chem. Soc.*, 1965, **87**, 395.

25 S. Lee, Y. You, K. Ohkubo, S. Fukuzumi and W. Nam, *Org. Lett.*, 2012, **14**, 2238.

26 (*a*) B. He and O. S. Wenger, *J. Am. Chem. Soc.*, 2011, **133**, 17027; (*b*) A. Staykov, J. Areephong, W. R. Browne, B. L. Feringa and K. Yoshizawa, *ACS Nano*, 2011, **5**, 1165.

27 R. G. Compton and C. E. Banks, *Understanding voltammetry*, Imperial College Press, London, 2nd edn, 2011.

28 D. H. Evans, *Chem. Rev.*, 2008, **108**, 2113.

29 A previous attempt to electrochemically distinguish both aryl-units of a DTE by nonsymmetrical substitution changed the location of the primary electron transfer, thus making clear conclusions difficult: see ref. 13*c*

30 T. Kubo, A. Shimizu, M. Uruichi, K. Yakushi, M. Nakano, D. Shiomi, K. Sato, T. Takui, Y. Morita and K. Nakasuji, *Org. Lett.*, 2007, **9**, 81.

31 A. J. Fry, *Electrochem. Commun.*, 2005, **7**, 602.

32 A. J. Fry, *Tetrahedron*, 2006, **62**, 6558.

33 C. Peng, P. Y. Ayala, H. B. Schlegel and M. J. Frisch, *J. Comput. Chem.*, 1996, **17**, 49.

 This journal is © The Royal Society of Chemistry 2013